

CaCO₃ (Calcite) Co-Doped with Eu and Cr: The Effect of Chromium/Europium Ratio on Blue Light Emission

E. E. Cervantes-Trujillo^{1,*}, S. A. Gómez-Torres^{1,*}, U. Caldiño², V. H. Lara-Corona³

¹Process and Hydraulic Engineering Department. Universidad Autónoma Metropolitana Campus Iztapalapa. Av. San Rafael Atlixco 186, Col. Vicentina 09340, CDMX, México.

²Physics Department. Universidad Autónoma Metropolitana Campus Iztapalapa. Av. San Rafael Atlixco 186, Col. Vicentina 09340, CDMX, México.

³Chemistry Department. Universidad Autónoma Metropolitana Campus Iztapalapa. Av. San Rafael Atlixco 186, Col. Vicentina 09340, CDMX, México.

*Corresponding author: E. E. Cervantes-Trujillo, email.: quiquenetocer@gmail.com ; S. A. Gómez-Torres, email: sgomez@xanum.uam.mx

Received November 26th, 2023; Accepted September 17th, 2024.

DOI: <http://dx.doi.org/10.29356/jmcs.v69i3.2185>

Abstract. The emission spectra of CaCO₃ co-doped with Eu and Cr have been studied in the UV-Vis region. A change in both the emission wavelength from 426 to 423 nm and the intensity, which is 30 times higher with respect to CaCO₃:Eu, indicates a significant modification of the optical properties of CaCO₃:Eu due to the influence of chromium (Cr/Eu = 0.5). Changes in the band gap (E_g) from 6 to 5.2 eV were observed when the material was calcined at 700 °C. This emission phenomenon was also observed at 600, 800 and 900 °C, but with lower intensity. Analysis of the excitation and emission bands indicates that Eu is in the 2+ oxidation state and Cr is in the 6+ oxidation state. This is because the emission occurs in the blue-violet region of the visible spectrum when exposed to UV light with a wavelength of 254 nm. The material has potential LED applications.
Keywords: CaCO₃:Eu-Cr; light emission; blueshift.

Resumen. Se estudiaron los espectros de emisión del CaCO₃ codopado con Eu y Cr en la región UV-Vis. Se observaron cambios en la longitud de onda de emisión de 426 a 423 nm y en la intensidad que resultó 30 veces mayor respecto a CaCO₃:Eu, lo que indica una modificación significativa en las propiedades ópticas de CaCO₃:Eu debido a la influencia del cromo (Cr/Eu = 0.5). Se observaron cambios en la energía de brecha (E_g) de 6 a 5.2 eV cuando el material se calcinó a 700 °C. Este fenómeno de emisión se observó también a 600, 800 y 900 °C, aunque con menor intensidad. El análisis de las bandas de excitación y emisión indica que el europio se encuentra en estado de oxidación 2+ y el cromo en estado de oxidación 6+. Esto se debe a que la emisión se produce en la región azul-violeta del espectro visible cuando se expone a una luz UV con una longitud de onda de 254 nm, por lo que el material puede tener aplicaciones potenciales como LED.

Palabras clave: CaCO₃:Eu-Cr; emisión de luz, corrimiento al azul.

Abbreviations

Bandgap Energy	(E_g)	Tetrahedral Symmetry	(C _{4v})
Calcite	(Cal)	Trigonal Symmetry Group	(R3c)
Charge Transfer	(CT)	Unit cell Volume	(V _{uc})

Comission Internationale de l'Éclairage	(CIE)	Ultraviolet Absorption spectrum	(F(R))
Conduction Band	(CB)	Ultraviolet-Visible spectrum	(UV-Vis)
Free Ion Energy	(E_{Afree})	Wavelength	(λ)
Metal-Ligand Charge Transfer	(MLCT)	Weight	(wt.)
Octahedral Symmetry	(O_h)	Valence Band	(VB)
Orthorhombic Symmetry Group	($Pm\bar{c}n$)	X-Ray Diffraction	(XRD)
Rare Earths	(RE)		

Introduction

Among the many compounds used for light emission in industrial, commercial, medical and other devices, $\text{CaCO}_3:\text{Eu}^{2+}$ is one of the most cost-effective materials due to its emission characteristics and chemical composition [1]. Luminescence is produced by exciting electrons that are transferred between the valence and conduction bands. This property is important because it indicates the range of wavelengths, from mid-IR to near-UV, at which a semiconductor can produce light emission. A fundamental requirement for the host material to exhibit photoluminescence in the visible region (380–750 nm) [2-4] is that the energy gap (E_g) exceeds 2.48 eV (500 nm). The crystal lattice of the compounds exhibiting this property can be doped in order to achieve emission. Consequently, a suitable host can permit the doping of the crystal lattice with lanthanides.

Calcium carbonate displays three primary spatial structures: Vaterite ($P6_3/mmc$, Unit cell Volume (V_{uc}) = 749 \AA^3 and $E_g = 4.4 \text{ eV}$), Aragonite ($Pm\bar{c}n$, $V_{uc} = 227 \text{ \AA}^3$ and $E_g = 1.0 \text{ eV}$) and Calcite ($R3c$, $V_{uc} = 368 \text{ \AA}^3$; $E_g = 6.0 \text{ eV}$) [2,3]. It is therefore recommended to avoid Aragonite formation due to its low E_g value. It is important to note that calcite possesses the highest E_g value. This is significant because it becomes a host for a dopant element which affects the energy required for an electron to move from the valence band (VB) to the conduction band (CB). If a dopant is a metal, electrons can be easily transferred from its last electronic shells to the host, resulting in the creation of "holes". This process involves electron borrowing and return between the host and the dopant. If a band-hopping electron generates a photon with sufficient energy to be in the visible region, light is produced. Consequently, calcite is regarded as a crucial host material. When doped with europium, which has an atomic radius of 204 pm and ionic radii of $\text{Eu}^{2+} = 125 \text{ pm}$, and $\text{Eu}^{3+} = 107 \text{ pm}$, the energy gap is reduced, resulting in the emission of photons in the visible region.

Previous research by Li *et al.* [1] demonstrated that incorporating Eu into CaCO_3 ($\text{CaCO}_3:\text{Eu}$) results in the emission of blue light at approximately 450 nm. This emission is attributed to the Eu^{2+} ion, although the synthesis of $\text{CaCO}_3:\text{Eu}^{2+}$ is complex because of the facile oxidation of Eu^{2+} to Eu^{3+} . Some studies have indicated that $\text{CaCO}_3:\text{Eu}^{3+}$ can be synthesized to achieve a more intense red emission at 625 nm [4,5].

This study presents a synthesis, characterization, and analysis of the luminescent behavior of $\text{CaCO}_3:\text{Eu}-\text{Cr}$. The selection of Cr as a codopant was based on its small ionic radius ($\text{Cr}^{2+} = 84 \text{ pm}$, $\text{Cr}^{3+} = 69 \text{ pm}$, and $\text{Cr}^{6+} = 52 \text{ pm}$), which suggests that it may have structural and electronic effects in $\text{CaCO}_3:\text{Eu}$ [6]. Furthermore, the incorporation of chromium may impede the oxidation of europium and impact the characteristic blue emission observed in the UV-Vis spectrum.

Experimental

A mixture of calcium chloride (99 % J. T. Baker), 1.5–0.5 mol% europium chloride hexahydrate (99.9 % Sigma-Aldrich), and 1.0–0.5 mol% chromium chloride hexahydrate (99.9 % Sigma-Aldrich) was prepared by mixing it with powdered charcoal in a 3:1 weight ratio of charcoal to calcium chloride. The resulting mixture was coprecipitated using deionized water and stirring at 400 rpm. The solid obtained was dried at 120 °C for 24 h, and finally calcined at 600, 700, 800, or 900 °C to promote the formation of CaCO_3 through a solid-solid reaction. The temperatures were selected to prevent Cr_2O_3 segregation below 600 °C and CaO formation above 900 °C. Additionally, the optimal calcination temperature for the greatest fluorescence emission intensity was identified, which was linked to a specific calcium carbonate structure. Vaterite (50–250 °C - V), calcite (460–

1000 °C - Cal), and aragonite (40–100 °C - A). X-ray diffraction (XRD) was performed using a Siemens D500 diffractometer to analyze the calcium carbonate (CaCO_3) species in the four $\text{CaCO}_3\text{:Eu-Cr}$ samples calcined at 600, 700, 800, and 900 °C. The objective was to identify the optimal structure for photoluminescence. The analysis of the XRD patterns was conducted using the software March! 3©. Ultraviolet-visible (UV-Vis) measurements were conducted on an Agilent Cary 5000 UV-Vis-NIR spectrophotometer within the wavelength range of 250 to 780 nm at a speed of 1 nm per second. Measurements of photoluminescence were performed on a Horiba Jobin Yvon Fluorolog® spectrophotometer with an excitation spectral range of 440 nm and an emission spectral range of 330 nm.

Results and discussion

X-Ray Diffraction (XRD)

The XRD patterns (Fig. 1) show the CaCO_3 species, which experience changes in intensity depending on the calcination temperature, relative to the prominent characteristic peaks of Calcite [Cal1 ($2\theta = 29.4$; $hkl = 104$), Cal2 ($2\theta = 39.4$; $hkl = 113$), Cal3 ($2\theta = 43.14$; $hkl = 202$)]. Furthermore, the sample calcined at 700 °C exhibited a greater quantity of synthesized CaCO_3 compared to the other samples, as illustrated in Fig. 1. While calcite is the dominant mineral, the March! 3© has detected small amounts of carbon (graphite at 26.5° and 54.7° in 2θ), CaO (at 32.4° and 64.7° in 2θ), and vaterite (CaCO_3 ; V at 27° in 2θ). It is noteworthy that Vaterite is capable of inducing a shift in the emission spectra towards the NIR region despite its low concentration due to its low E_g value (1 eV). CaO presents a challenge for Eu and/or Cr doping, despite its appropriate E_g (6.25 eV), because of its small unit cell volume of only 28.3 \AA^3 , which leaves no interstitial sites or structural integration options. Graphite is a residue resulting from the charcoal reaction, which is employed to enhance the generation of calcium carbonate.

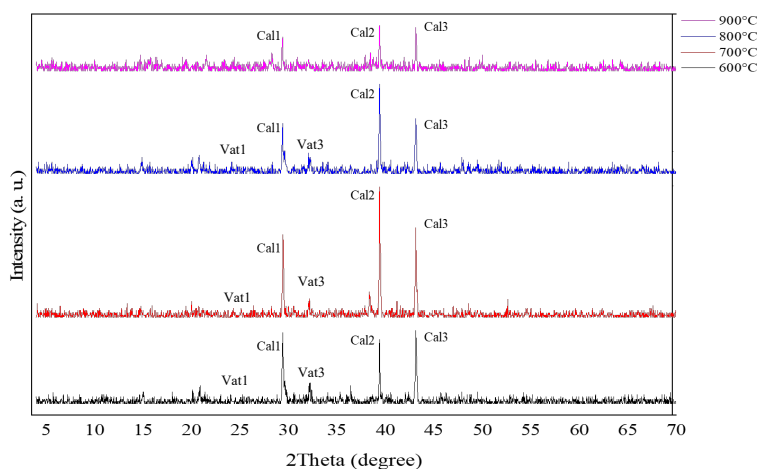


Fig. 1. XRD patterns of the samples that were calcined at 600 (---), 700 (----), 800 (---), and 900 °C (----). The characteristic peaks of calcite: Cal1 to (104), Cal2 to (113), and Cal3 to (202), and Vaterite: Vat1(102), Vat3 (006) are shown for each temperature.

Table 1 illustrates that the composition of calcite exceeds 55 wt.% in almost all samples. However, the sample calcined at 700 °C exhibits the highest composition, reaching 86.3 wt.%, which subsequently decreases to 56.7 wt.% following calcination at 900 °C. Furthermore, both the levels of graphite (C) and calcium oxide (CaO) increase with increasing calcination temperature, while the levels of vaterite decrease and eventually disappear at 800 °C. Less than 1.5 wt% of other compounds are also observed as a function of temperature, including calcium carbide (CaC_2) at 800 and 900 °C and in an amount less than of 0.5 % europium chloride (EuCl_3) at 600 °C. The

presence of water, due to the hygroscopic nature of calcium carbonate, is attributed to some low-intensity peaks in 2θ [7]. The thermodiffraction analysis depicted in Fig. 2 was then conducted to ascertain the formation of CaCO_3 , circumventing the influence of adsorbed water. The specimen utilized for the thermodiffraction analysis was an uncalcined sample procured from a hydrothermal synthesis, which was evacuated at 10^{-3} torr and heated in situ from 25 to 800 °C at a heating rate of 10 °C/min. The presence of the calcite crystal structure as a function of temperature is illustrated in Fig. 2. The behavior of calcite wt.% vs. temperature is depicted in the inset at the top right of Fig. 2. It can be observed that the calcite wt.% is greater than 80 % from 400 °C onwards.

Table 1. Composition (wt.%) of the samples obtained from the analysis of the XRD patterns of Fig. 1 using the software March! 3©.

Temperature (°C)	Species (wt.%)			
	Calcite (CaCO_3)	Graphite (C)	Vaterite (CaCO_3)	Calcium Oxide (CaO)
600	78.3	4.1	7.6	0.5
700	86.3	13.0	1.0	0.7
800	63.6	20.1	0.6	4.4
900	56.7	21.3	0	17.7

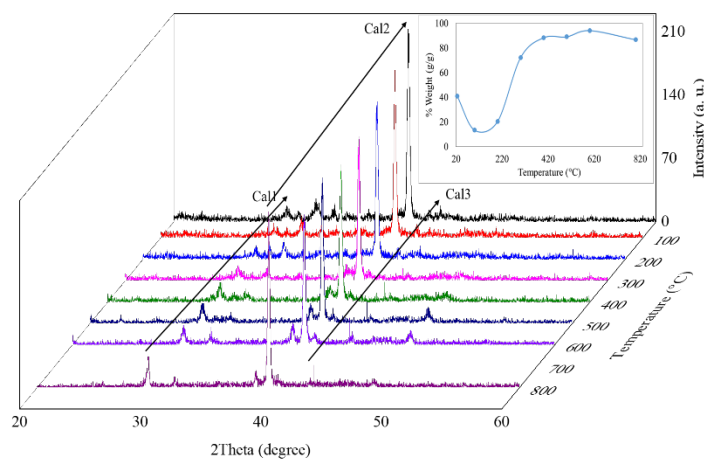


Fig. 2. Thermodiffraction of the sample of CaCl_2 , C, and Eu and Cr salts, at 10 °C/min under vacuum (10^{-3} torr).

The theoretical and experimental calcite unit cell volume has been established for the $R3c$ space group at 382.37 \AA^3 [8]. However, it should be noted that there are temperature-dependent structural changes. In the range of calcination temperatures used in this study, V_{uc} exhibits a slight increase between 600 and 800 °C. However, the most significant change occurs at 900 °C, where V_{uc} increases and the wt.% of calcite drops to 56 % (Table 1 and 2). The increase in V_{uc} relative to the ideal CaCO_3 unit cell [8] is 3.8 % at 700 °C (Table 2). If the sum of the molar percentages of Eu and Cr is considered to be 1.5 % (Eu 1 %, Cr 0.5 %), then the increase in V_{uc} is within the expected values. The linear increase of V_{uc} with temperature was tested using the Vegard's law, which is a direct relationship between the crystal lattice parameters and the amount of dopant. This

relationship can be expressed as $a = a_1(1-x) + a_2(x)$, where a_1 is the host parameter, a_2 is the dopant parameter, and x is the mole fraction of the dopant. Additionally, the effect of thermal expansion of some of the unit cell parameters (a , c) was considered [8]. Fig. 3 displays three curves, each one representing a distinct data set. The first curve (a) encompasses the data obtained in this study, the second (b) represents the reference data, and the third (c) is the result of calculations performed using Vegard's law. The parameter a exhibits a slight increase between 600 and 800 °C, but at 900 °C, it declines. For both the reference data (\blacktriangle) and the data calculated with Vegard's law, the observed data deviates from the ideal values (\bullet) by 0.25 % more than the reference data. This is particularly evident for parameter c , where the observed data (\blacklozenge) differs from the reference data ($+$) by a greater margin, with smaller dimensions and a maximum difference of 3.8 % at 700 °C [9]. The results of parameters a and c have direct effects on the unit cell volume (Fig. 3(c)), which resulted in a lower observed volume (\blacklozenge) than that of the reference (\bullet). The concentration of both Eu and Cr barely reaches 1.5 mol% with respect to Ca. This concentration is low enough to cause a noticeable change in the XRD peaks of calcite. It can be postulated that the observed decrease in V_{uc} is related to a thermal effect, given that the difference between the reference volume and the observed volume is approximately 0.65 %, which is indicative of the removal of defects in the crystalline structure. The thermal degradation of calcium carbonate is a natural process, occurring through the decarbonization reaction with oxygen, which forms calcium oxide and carbon dioxide. This process results in a change in the CO-Ca bonds and their orientation as the calcination temperature increases, reaching a critical change at 700 °C, as evidenced in references [9,10].

Table 2. Volume of unit cells (V_{uc}) of calcite in $\text{CaCO}_3:\text{Eu-Cr}$ samples calcined at different temperatures.

T (°C)	V_{uc} (\AA^3)	ΔV_{uc}^* (%)
600	366.58	4.13
700	367.76	3.82
800	368.2	3.7
900	374.74	1.99

* ΔV_{uc} Calculated with respect to $V_{uc} = 382.37 \text{ \AA}^3$ [7].

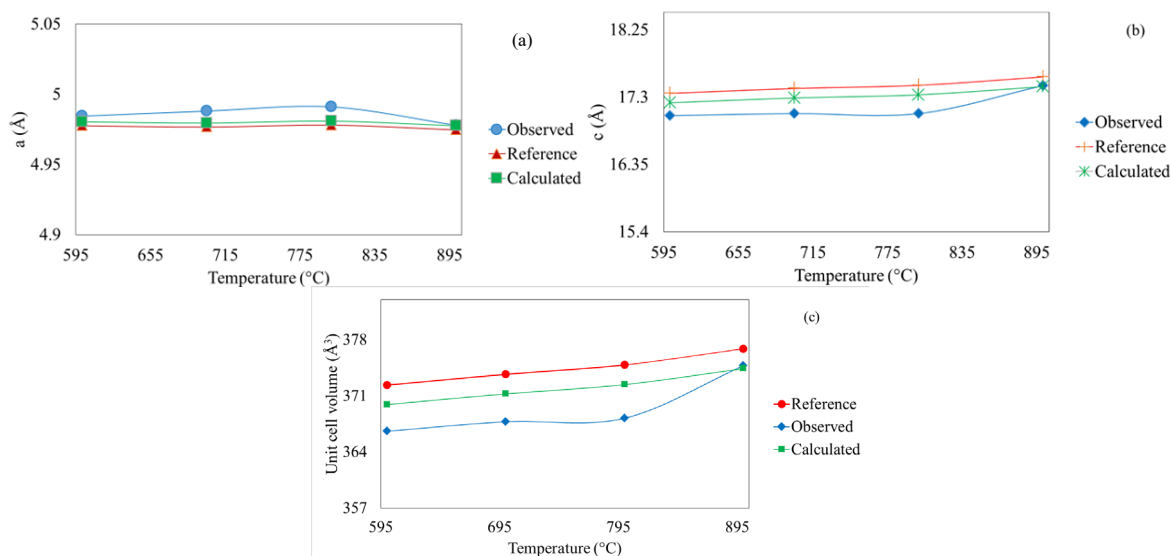


Fig. 3. Thermal effect change curves of parameter a (a), parameter c (b), and unit cell volume (c) for $\text{CaCO}_3:\text{Eu}$ 1 %, Cr 0.5 % of space group $R3c$.

Fluorescence spectroscopy (Emission and excitation)

Fig. 4 depicts the visible emission spectra of $\text{CaCO}_3\text{:Eu-Cr}$ samples with varying Cr/Eu ratios and calcined at distinct temperatures. Additionally, samples $\text{CaCO}_3\text{:Eu}$ and $\text{CaCO}_3\text{:Cr}$ prepared as a reference material are included for comparison. The four samples with identical concentrations of 1/2-Cr/Eu exhibited alterations in the emission band between 380 and 530 nm as a function of calcination temperature. Since the 4f electronic levels have minimal interaction with the surrounding crystal field, the emission energy remains consistent regardless of the host. In contrast, the electrons in the 5d level interact with the rare earth (RE) bound anions, rendering them susceptible to the influence of the surrounding crystal field. This phenomenon is observed in the excitation and emission bands of the 5d levels, which are considerably broader than those of the 4f levels [11]. Consequently, both emission and excitation are dependent on the host and the lanthanide. In the case of the $\text{CaCO}_3\text{:Eu}$ system, where Eu^{2+} is immersed in the crystal structure with ions such as O^{2-} , C^{4+} and Ca^{2+} , and the electronic transfer $f^65d^1 \rightarrow 4f^7(^8S_{7/2})$ that causes the emission of allowed dipole and spin df [12]. The reported emission band for Eu^{2+} in $\text{CaCO}_3\text{:Eu}$ is approximately 450 nm [1], and according to some reports [12, 13], it should produce a redshift of the emission band when $\text{CaCO}_3\text{:Eu}^{2+}$ is co-doped with another element. However, our study system contains chromium, and the emission band is not redshifted but blueshifted (Fig. 4). The emission band was observed at 423 nm, and only the Eu-doped sample exhibited emission at 426 nm, which was 27 nm lower than the emission reported by Li et al. [1], and 26 nm higher than that reported by Tanguy et al. [14], who found an emission band at 397 nm using CaLiF_3 as a host. However, in our samples, there was a notable change in intensity when calcite was doped with Eu, with a markedly higher intensity observed when it was codoped with Eu and Cr. This suggests that Eu^{2+} is positioned at Ca sites within the structure.

It is notable that in both cases, the literature indicates that Eu^{2+} exhibits $4f^65d^1$ type transitions and an ionic radius of 125 pm, suggesting that the interaction with the host crystal field should be robust. Given that Ca^{2+} has an ionic radius of 100 pm, Eu^{2+} could potentially be accommodated in a calcium site, a straightforward process due to its radial dimensions. In contrast, the impact of Cr is not yet fully understood. Studies indicate that the excitation band for Cr^{3+} (ionic radius = 61 pm) is situated between 530 and 745 nm, contingent on the host, while the emission band is situated between 1100 and 1400 nm [15]. The $^4T_{2g} \rightarrow ^4A_{2g}$ and $^4T_{2g} \rightarrow ^4T_{1g}$ transitions arise from a special case in which the antibonding electrons from the $^4A_{2g}$ ground state are promoted to higher energy states such as T, which are also crystal field sensitive. These bands are not observed in the spectra of Fig. 4. However, there is a possibility that they may be detected through an ionic Cr^{6+} phase with an excitation band at 290 nm [4, 16]. In this case, this could represent the E_g shift of calcite, which would modify the UV absorption bands. Another compound that contains Eu^{2+} and exhibits an emission band similar to that reported in this work is CaLiF_3 , with an emission band at 397 nm and an excitation band at 364 nm [14].

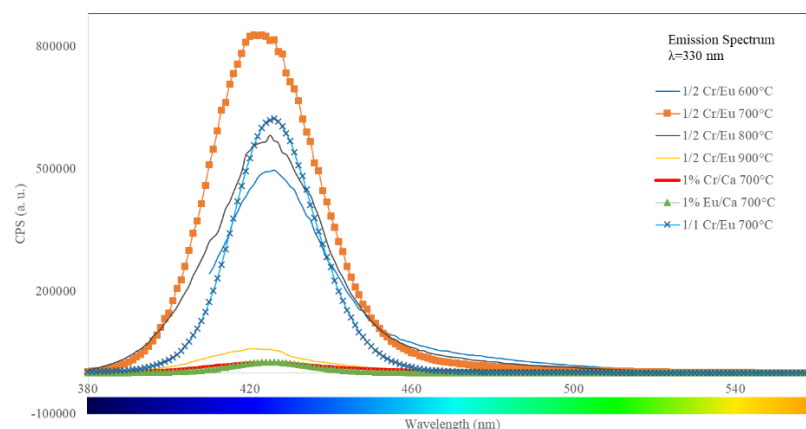


Fig. 4. Visible photoluminescence spectra for $\text{CaCO}_3\text{:Eu-Cr}$ compounds calcined at different temperatures and with different Cr/Eu molar ratios.

Fig. 5 illustrates the excitation spectra, wherein the maximum excitation band for the four $\text{CaCO}_3\text{:Eu-Cr}$ samples is observed at 364 nm. Subsequently, Equation (1) was employed to calculate the redshift of the

emission

band

[13]:

$$E_{em}(n, Q, A) = E_{Afree}(n, Q) - D(Q, A) - \Delta S(Q, A) \quad (1)$$

E_{Afree} is the ionization free energy of a lanthanide in the gaseous state. $D(Q, A)$ is the term used to determine the energy of the first 5d level and the redshift. $\Delta S(Q, A)$ is derived from the Stokes shift $S(Q, A)$, which represents the maximum difference between the excitation and emission bands. The parameter A represents the host effect for redshift, while Q denotes the ionized state of the lanthanide ($1+$, $2+$, $3+$, ...). The Dorenbos data for Eu^{2+} doped CaCO_3 , with $D = 10190 \text{ cm}^{-1}$ and $\Delta S = 1587 \text{ cm}^{-1}$ [Dorenbos, 2003], have been employed in the calculations. According to Equation 1, the emission at 423 nm (23640 cm^{-1}) yields an E_{Afree} value of 35417 cm^{-1} (282.34 nm). In consideration of the disparate values for Eu^{2+} -doped compounds, as presented by Dorenbos [13], it can be concluded that the E_{Afree} excitation band is situated within these values (364 nm). However, in terms of excitation energy, it is relatively low in comparison to the previously reported value of 350 nm [1]. It is therefore necessary to investigate the impact of Cr on the structure of CaCO_3 must be investigated, as no emission or excitation band has yet been identified that can elucidate its influence on the crystalline system.

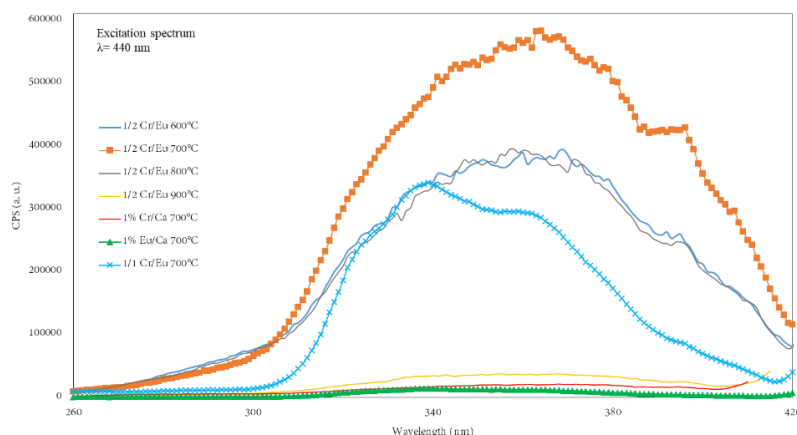


Fig. 5. Excitation spectra for $\text{CaCO}_3:\text{Eu-Cr}$ compounds calcined at different temperatures and with different Cr/Eu molar ratios.

As previously stated, there is a paucity of documented data pertaining to the excitation and emission bands of Cr ionic species in a complex crystalline system such as the one under investigation here. Samples were thus synthesized with an inverse Cr/Eu ratio to that previously employed, namely Eu 1% - Cr 0.5% ($\text{Cr/Eu} = 0.5$), Cr 1% - Eu 1% ($\text{Cr/Eu} = 1$), and Eu 0.5% - Cr 1% ($\text{Cr/Eu} = 2$). The results demonstrate that the emission and excitation spectra of $\text{CaCO}_3:\text{Eu-Cr}$ with Eu 1% and Cr 0.5% exhibit the most intense emission (Fig. 6(a) and 6(b)). The emission intensity is observed to be 32 times higher when less chromium is present and 30 times higher when europium is the sole dopant. This indicates that the emission due to chromium is minimal. Furthermore, when comparing the excitation spectra, a similar behavior to the emission spectra is observed, *i.e.*, there is a reduction in the UV excitation band, with a 28-fold smaller difference when more Cr is present [Fig. 6(b) right axis (0.5 Cr/Eu; 1.0 Cr/Eu); left axis (1% Cr/Ca; 1% Eu/Ca)]. A broad band between 250 and 310 nm is observed only in the 1% Cr sample (Fig. 6(b)). Two absorption bands at 280 and 370 nm belonging to Cr^{6+} are mentioned in the work of Wang et al. [16]. Accordingly, the band observed between 250 and 310 nm depends on the Cr concentration in the sample and can be attributed to Cr^{6+} . This observation indicates a contribution of chromium to the absorption of radiation by calcium carbonate, which must indirectly cause the blueshift of the light emission. Furthermore, the excitation band belonging to Eu exhibits a behavior of absorption UV radiation at 339 nm when there is a higher concentration but a lower emission. The most

significant discovery to emerge from the study of Cr and Eu in CaCO₃, is that a low molar percentage of Cr, which is always accompanied by Eu in a major count, gives the best emission blue (423 nm).

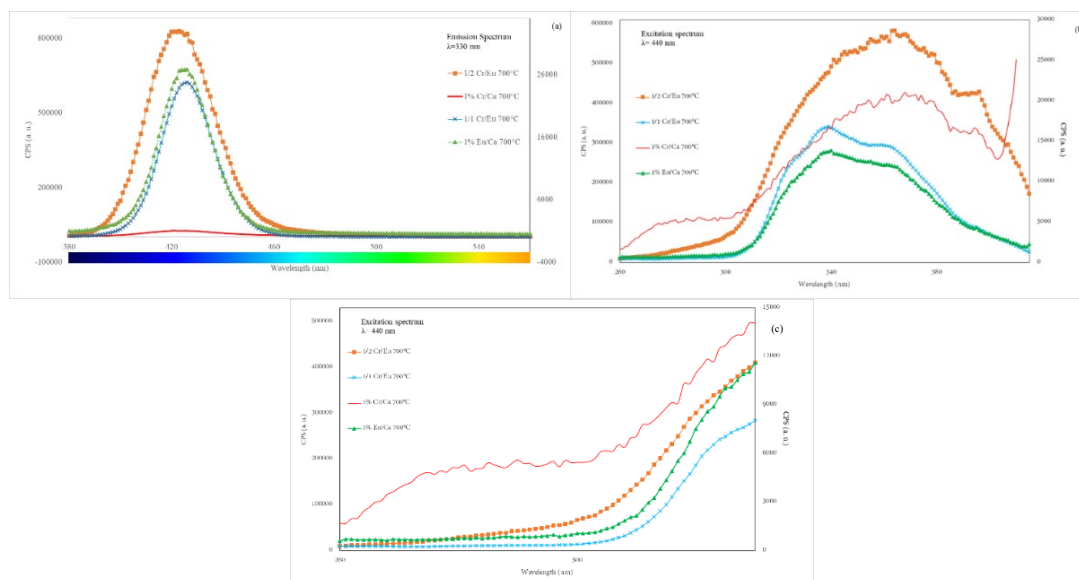


Fig. 6. Emission spectra (a), excitation spectra (260–405 nm) (b), and excitation spectra (260–340 nm) (c) for CaCO₃:Eu-Cr compounds with different Cr/Eu molar ratios and calcined at 700 °C.

UV absorption spectrum (F(R)) [Kubelka-Munk]

Calcium carbonate exhibits a direct transition allowed [17]. Equation (2) was employed to determine the energy of the absorption edge [17]:

$$E_{opt} = (h\nu \cdot F(R))^{1/\eta} \quad (2)$$

The Planck constant (h), the frequency of the wavelength (ν), and the value of 2 for an allowed direct transition (η) are fundamental parameters in the calculation of the gap energy (E_g). The latter can be determined by plotting E_{opt} against E and identifying the intercept on the E axis as an approximation of the downward slope of the curve, which represents the transition from high to low energy.

Fig. 7 illustrates the curves utilized to compute the E_g for the CaCO₃:Eu 1 %-Cr 0.5 % samples subjected to calcination at 120, 600, 800, 900 °C (depicted on the left vertical axis) and at 700 °C (depicted on the right vertical axis). The computed E_g values are presented in Table 3. It is evident that there are notable discrepancies between the E_g values at each temperature. Nevertheless, they are comparable to those anticipated for the existing calcium carbonate structures and those reported by Hossain et al. [3].

It is noteworthy that the values obtained for E_g fall within the range of 6.00 to 5.07 eV. The former is obtained in the UV region, while the latter is the value of the indirect transition calculated with numerical methods and software [18]. The change in E_g is ascribed to the presence of Cr⁶⁺, which does not impede light emission. This results in a shift in the manner by which the material absorbs radiation, thereby enabling emission through Eu²⁺ towards an emission that is closer to the UV region.

An E_g of 6 eV (206.6 nm) corresponds to undoped calcium carbonate. In regard to the fluorescence results, it can be observed that Cr⁶⁺ is excited at 4.27 eV (290 nm) while Eu²⁺ is excited at 3.41 eV (364 nm). Moreover, the redshift calculated from Equation (1) yielded an E_{Afree} value of 35417.6 cm⁻¹ (282.3 nm). It is noteworthy that a redshift error of 567 cm⁻¹ was previously reported for CaCO₃:Eu²⁺ [16], which places the excitation band at 286.9 nm, within the observed Cr⁶⁺ band.

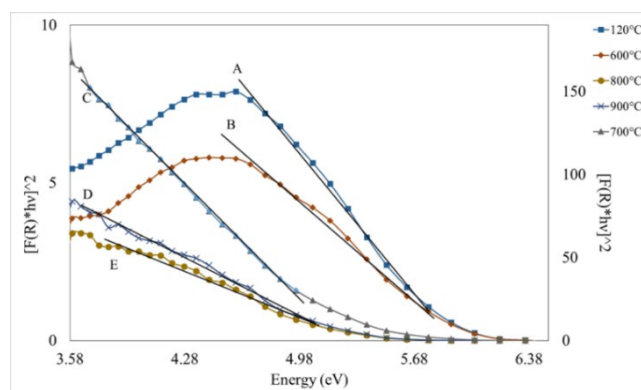


Fig. 7. Absorption edge energy for CaCO_3 samples calcined at 120, 600, 800, and 900 °C, and $\text{CaCO}_3\text{:Eu 1\%, Cr 0.5\%}$ calcined at 700 °C (right axis). Lines A, B, C, D, and E correspond to the approximations of E_g for each compound synthesised.

Table 3. CaCO_3 compounds doped with 1 % Eu and 0.5 % Cr, with gap energy variation due to thermal effect.

Calcination Temperature (°C)	E_g (eV)
120	5.91
600	5.96
700	5.23
800	5.24
900	5.28

The significance of Cr is also evident in Fig. 8, where the absorption bands of CaCO_3 doped with 1 % Eu and 0.5 % Cr (---) and with 0.5% Eu and 1% Cr (---) are compared. At higher Cr concentrations, the absorption bands become more pronounced, indicating transitions within an octahedral binding field. The first band is observed at 370 nm (${}^1A_{1g} \rightarrow {}^5T_{2g}$) ($t_{2g}^4 e_g^2 \leftarrow t_{2g}^6$). In this case, there is a multiplicity of 4 with 2 unpaired electrons. The second absorption band, observed at 270 nm, ${}^1T_{2g} \leftarrow {}^1A_{1g}$, is attributed to the transition from a low-spin $t_{2g}^5 e_g^1$ orbital to a high-spin t_{2g}^6 orbital. This transition is described in detail in reference [19].

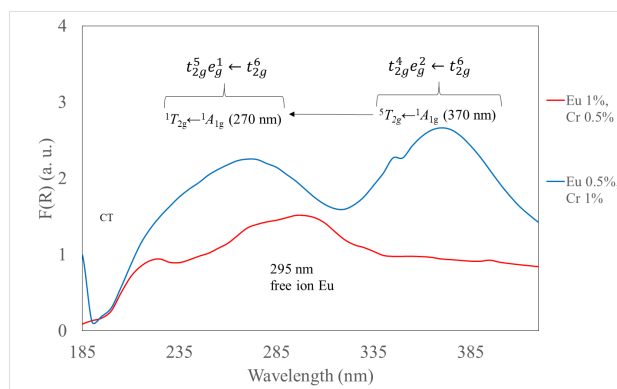


Fig. 8. $F(R)$ UV absorption spectra (185–390 nm) for $\text{CaCO}_3\text{:Eu 1\%, Cr 0.5\%}$ (---), and $\text{CaCO}_3\text{:Eu 0.5\%, Cr 1\%}$ (---).

Fig. 9 depicts the Tanabe-Sugano diagram, which was generated using the simulator developed by Lancashire [20], and the absorption bands (270 and 370 nm) derived from the UV spectra. The ratio between the bands at 370 and 270 nm was calculated to search in the Tanabe-Sugano diagram (Fig. 9) for the value of Δ_0/B , which was then used to determine the B value (Racah parameter) to identify the probable transitions occurring during UV excitation. The transitions obtained correspond to the allowed transitions. Forbidden transitions are excluded from consideration because the intersections do not correspond to the forbidden transition curves in the Tanabe-Sugano diagram (Fig. 9). Table 4 presents the most pertinent data obtained from the band ratio, 1.37 (ν_2/ν_1), bands observed in Fig. 8 and their relationship with the Racah parameters for the free Cr^{6+} ion, $B = 1080 \text{ cm}^{-1}$ and $C = 4774 \text{ cm}^{-1}$. These data are crucial for recalculating the crystalline octahedral system of Cr with six CO ligands (Table 4).

The Racah parameters are lower due to the influence of the CO ligands on the Cr^{6+} energy. Conversely, if the nephelauxetic parameter (β), which is calculated as $\beta = B_{\text{complex}}/B_{\text{Free ion}}$, is < 1 , it indicates that the metal-ligand bonds are covalent, with a reduced electron-electron repulsion. The results demonstrate that this occurs in the case of the crystalline system CaCO_3 : Eu-Cr.

A weak charge transfer (CT) effect is also observed after 190 nm (Fig. 8), as well as a shoulder at 345 nm corresponding to a reduction in $\text{O}_h \rightarrow \text{C}_{4v}$ symmetry. When Eu is at 1 % concentration, its most relevant absorption is found at 295 nm, with a band similar to that of the free ion [13], covering the chromium bands. Nevertheless, minor peaks are discernible at 270 and 370 nm (Fig. 8), indicative of the influence of CO in the solid system. This is due to the fact that CO is a robust electron acceptor ligand that gives rise to the metal-ligand charge transfer (MLCT) effect [21]. As the π bonds possess empty orbitals that can accommodate the transferred electrons, and as these bonds are more energetic, the energy splitting of the crystal field also increases.

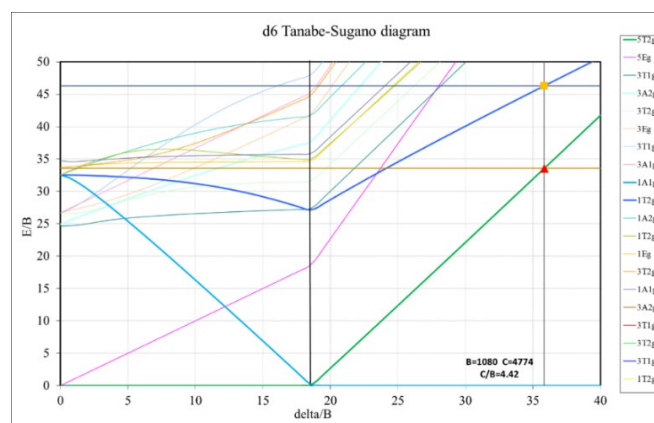


Fig. 9. Octahedral configuration Tanabe-Sugano diagram for 270 and 370 nm bands in cm^{-1} of Cr (d^6), with $\nu_2/\nu_1 = 1.37$. The thick curves blue and green represent the allowed transitions.

Table 4. Data recalculated from Fig. 9 and absorption bands observed in Fig. 8 when Cr concentration is 1 %.

P. Racah B (cm^{-1})	802.69
P. Racah C (cm^{-1})	3547.89
ν_1	46.29
ν_2	33.56
Δ/B	35.833
$10 \Delta q$ (cm^{-1})	28762.85
β	0.7432

Fig. 10 illustrates the process of electron transfer. It begins by showing how the E_g of calcite with its direct allowed transition behaves when doped with Eu and Cr. The E_g decreases towards the value of the indirect gap (5.07 eV). Electron transfer in the dopants occurs within the E_g values, so different combinations can occur. The dominant dopant is Eu, since the higher the concentration, the higher the luminescence. Accordingly, the transfer may occur from Eu to the CaCO_3 holes, then to Cr^{6+} , then back to Eu^{2+} , and finally emit blue light (Fig. 10(c)). An alternative, more straightforward pathway is illustrated in Fig. 10(b). Here, excitation causes electrons to pass through CaCO_3 via Cr, move to Eu, and then emit light.

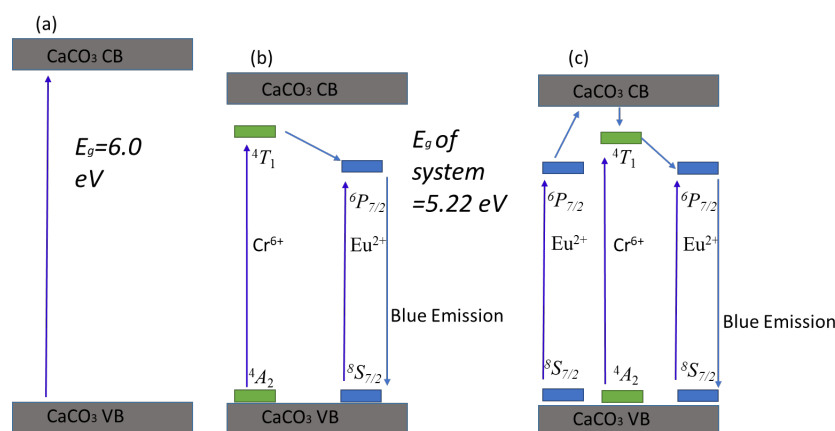


Fig. 10. Example of the activation of rare earths and their effect on CaCO_3 , with Eu and Cr as the activators, for the particular case of greater luminescence (sample calcined at 700°C). **(a)** The undoped calcite gap energy is shown, **(b)** Once the calcite is doped, E_g decreases and the simple electronic transfer begins, where Cr absorbs the photons and the excited electrons are transferred to Eu, emitting blue light. **(c)** The other way in which the electrons are transferred is to first excite the electrons from Eu, then they are transferred to the holes of the CaCO_3 , these electrons pass to Cr and finally return to Eu to emit blue light.

Color detection in the Visible spectrum (Vis)

During the light emission of the calcined CaCO_3 :Eu-Cr compounds, spectroscopic analysis in the visible region (Vis) was carried out in an Agilent Varian 5000 UV-Vis-NIR spectrophotometer using a xenon lamp. The spectra are shown in Fig. 11. The percentage reflectance of the doped CaCO_3 is greater than 55 %, indicating that the samples can be described as light grey to white compounds. In the wavelength region below 450 nm, the spectra curves exhibit a slight increase, not exceeding 6 %. This phenomenon is more evident in the sample that has been calcined at 900°C , as its reflectance is between 60 and 66 %, which presents as a whitish compound.

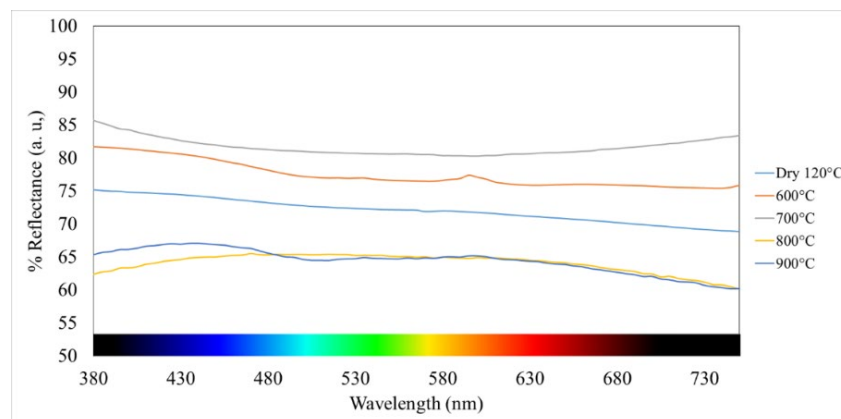


Fig. 11. Visible spectra of CaCO_3 doped with Eu 1 % and Cr 0.5 % dried at 120°C , and calcined at 600, 700, 800, and 900°C .

The spectra were reinterpreted using the CIE 1931 algorithm [22]. The data demonstrate that the luminescence of the five compounds, recorded with a xenon lamp in the visible region (Fig. 12), is concentrated at coordinates $x = 0.31$ and $y = 0.33$ (●), which are in close proximity to the unsaturated center of the color. This indicates that visible light does not excite the compound, as evidenced by its superimposition on the CIE 1931 color spectrum diagram (Fig. 12). This indicates that the compounds exhibit a color that is similar to white.

The opposite happens when the compound $\text{CaCO}_3:\text{Eu-Cr}$ is exposed to UV light at 254 nm. Fig. 12 shows the image of the compound calcined at 700 °C. The position of the four compounds calcined at 600, 700, 800 and 900 °C is at the bottom of the CIE 1931(■) diagram (Fig. 12), at $x = 0.15$ and $y = 0.10$. These coordinates are in the deep blue region, with a 470 nm blue color purity of 85 % [23], confirming the behaviour of the emission by direct excitation with a UV lamp.

Li and colleagues [1] are the only researchers to have discovered the effectiveness of an Optical Brightness Agent (OBA) containing europium (in the form of Eu^{2+}) in brightening paper, as part of a review of studies on CaCO_3 and Eu. The light emitted has a wavelength of 450 nm. However, the problem with using europium is its tendency to undergo a moisture-dependent change from Eu^{2+} to Eu^{3+} , resulting in a loss of luminescence. Therefore, chromium was considered a favourable co-dopant to increase stability and improve light emission efficiency. The results show a blue shift from 450 to 425 nm. However, the compound remains hydrophilic and its emission is affected by humidity, making it a suitable LED compound for use in a vacuum or with noble gases. Initial results indicate a weak resistivity response to an electric current of 100 volts under vacuum conditions, while no response is observed for Eu, Cr or CaCO_3 at other currents.

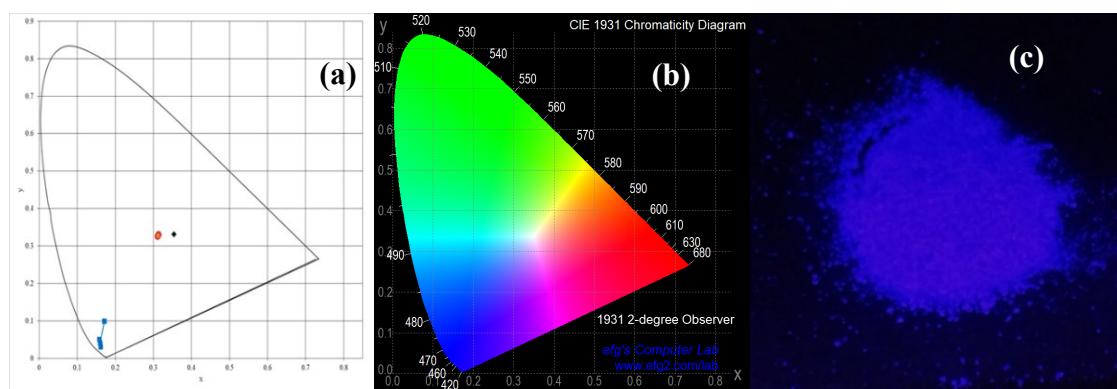


Fig. 12. (a) Color localization for $\text{CaCO}_3:\text{Eu-Cr}$ samples calcined at 600, 700, 800 and 900 °C without excitation with UV light (●), (b) CIE 1931 diagram, and (c) Image of $\text{CaCO}_3:\text{Eu-Cr}$ calcined at 700 °C and excited at 254 nm.

Conclusions

The structure of CaCO_3 characterised by XRD and thermal diffraction, confirmed the $R3c$ structure in a trigonal rhombohedral crystal system with a central Ca atom and six ligands of the CO_3 group. This indicates a strong crystalline field or even stronger than CN^- . Since the atomic radius of Ca for coordination 6 is 100 pm, although smaller than that of Eu (117 pm), the substitution of Ca for Eu in the crystal lattice is facilitated. Using the luminescence theory discussed by Bünzli [24], it was determined that metal-ligand charge transfer (MLCT) is likely to occur by electron transfer from Eu to the carbonate ligand. This is consistent with the experimental evidence provided by fluorescence spectroscopy, which shows that Eu is the driver of light emission, influenced by the surrounding crystal field. In other words, a strong ligand (electroattractant), in this case the CO_3 ligand, attracts the e-stealing Eu.

The light emission behaviour of 1/2 Cr/Eu CaCO_3 calcined at 700 °C showed the most intense emission and a light blue shift from 426 to 423 nm with respect to $\text{Eu}:\text{CaCO}_3$ also calcined at 700 °C. An effective shift of 3 nm results in the absence of Cr emission bands. However, there are excitation bands associated with the chromium absorption bands, such as 290 and 368 nm, are present, although these are obscured by the Eu and

CaCO₃ bands for samples with 1 % Eu. At a concentration of 1% Cr, the aforementioned absorption bands are revealed, resulting in a sacrifice of emission. However, this demonstrates the action of the compound upon UV radiation excitation due to the energy generated by the splitting of the binding field and the electronic repulsion it generates. Nevertheless, an elevated concentration of Cr results in the extinguishing of light emission. The shift of the gap energy between 5.94 and 5.22 eV depends on the calcination temperature. It is evident that there have been alterations in the optoelectronic properties of CaCO₃. The initial value for calcite is 6.0 eV. It can thus be concluded that the observed effect is due to the presence of Eu and Cr, as well as the higher amount of calcite at 700 °C.

The CaCO₃:Eu-Cr compound displays promising characteristics as a light-emitting material, particularly in LED applications. Additionally, it serves as an illustrative case study for investigating the relationship between dopants of varying periods (Ln-Ln or transition metal-metal) which are influenced by the surrounding bonding field. This field exerts an influence on the other dopant, resulting in the production of a luminescence effect.

Acknowledgments

E. E. Cervantes-Trujillo would like to thank CONACyT for the scholarship granted for his postgraduate studies. The authors thank the Universidad Autónoma Metropolitana - Iztapalapa, México, for funding and supporting the project.

References

1. Li, W. M.; Hänninen, T.; Leskelä, M.; Saari, J.; Hase, A. *J. Alloy. Compd.* **2001**, 323-324, 236–238. DOI: [http://dx.doi.org/10.1016/s0925-8388\(01\)01050-7](http://dx.doi.org/10.1016/s0925-8388(01)01050-7).
2. Weir, C. E.; Lippincott, E. R. *J. Res. NBS. A Phys. Ch.* **1961**, 65, 173. DOI: <http://dx.doi.org/10.6028/jres.065a.021>.
3. Hossain, F. M.; Murch, G. E.; Belova, I. V.; Turner, B. D. *Solid State Commun.* **2009**, 149, 1201–1203. DOI: <http://dx.doi.org/10.1016/j.ssc.2009.04.026>.
4. Kowalska, K.; Kuwik, M.; Polak, J.; Pisarska, J.; Pisarski, W. A. *Materials.* **2021**, 14, 7156. DOI: <http://dx.doi.org/10.3390/ma14237156>.
5. Zhou, B.; Liu, B.; Zou, H.; Song, Y.; Gong, L.; Huo, Q.; Xu, X.; Sheng, Y. *Colloids Surf., A.* **2014**, 447, 166–171. DOI: <http://dx.doi.org/10.1016/j.colsurfa.2013.12.078>.
6. Tamatani, M., in: *Principal phosphor materials and their optical properties*, 2nd ed.; Phosphor Handbook, CRC/Taylor and Francis, **2007**, 178–182.
7. López-Arce, P.; Gómez-Villalba, L.S.; Martínez-Ramírez, S.; Álvarez de Buergo, M.; Fort, R. *Powder Technol.*, **2010**, 205, 263–269. DOI: <http://dx.doi.org/10.1016/j.powtec.2010.09.026>.
8. Graf, D. L. *Am. Mineral.* **1961**, 46, 11-12.
9. Dove, M. T.; Powell, B. M. *Phys. Chem. Miner.* **1989**, 16. DOI: <http://dx.doi.org/10.1007/bf00197019>.
10. Ishizawa, N.; Setoguchi, H.; Yanagisawa, K. *Sci Rep-UK.* **2013**, 3. DOI: <http://dx.doi.org/10.1038/srep02832>.
11. Dorenbos, P. *J. Lumin.* **2000**, 91, 91–106. DOI: [http://dx.doi.org/10.1016/s0022-2313\(00\)00197-6](http://dx.doi.org/10.1016/s0022-2313(00)00197-6).
12. Dorenbos, P. *J. Lumin.* **2003**, 104, 239–260. DOI: [http://dx.doi.org/10.1016/s0022-2313\(03\)00078-4](http://dx.doi.org/10.1016/s0022-2313(03)00078-4).
13. Dorenbos, P. *J. Phys-Condensed Mat.* **2003**, 15, 575–594. DOI: <http://dx.doi.org/10.1088/0953-8984/15/3/322>.
14. Tanguy, B.; Merle, P.; Pezat, M.; Fouassier, C. *Mater. Res. Bull.* **1974**, 9, 831–836. DOI: [http://dx.doi.org/10.1016/0025-5408\(74\)90119-6](http://dx.doi.org/10.1016/0025-5408(74)90119-6).
15. Aboshyan-Sorgho, L.; Cantuel, M.; Petoud, S.; Hauser, A.; Piguët, C. *Coordination Chem. Rev.* **2012**, 256, 1644–1663. DOI: <http://dx.doi.org/10.1016/j.ccr.2011.12.013>.

16. Wang, D.; Zhang, X.; Wang, X.; Leng, Z.; Yang, Q.; Ji, W.; Lin, H.; Zeng, F.; Li, C.; Su, Z. *Crystals*. **2020**, *10*, 1019. DOI: <http://dx.doi.org/10.3390/cryst10111019>.
17. Barton, D. G.; Soled, S. L.; Iglesia, E. *J. Phys. Chem.* **1999**, *6*, 87–99. DOI: <http://dx.doi.org/10.1023/a:1019126708945>.
18. Medeiros, S. K.; Albuquerque, E. L.; Maia, F. F.; Caetano, E. W. S.; Freire, V. N. *J. Phys. D Appl. Phys.* **2007**, *40*, 5747–5752. DOI: <http://dx.doi.org/10.1088/0022-3727/40/18/036>.
19. Atkins, P. W.; Shriver, D. E.; Overton, T.; Rourke, J.; Weller, M.; Armstrong, F., in: *Inorganic Chemistry*, 4th ed.; McGraw Hill, **2008**, *19*, 473.
20. http://wwwchem.uwimona.edu.jm/lab_manuals/CrTSexptnu/TSD3.html, accessed in August 2022.
21. Adachi, C.; Tsutsui, T., in: *Fundamentals of luminescence*, 2nd ed.; Phosphor Handbook, CRC/Taylor and Francis, **2007**, 66–69.
22. Nassau, K., in: *Color for Science, Art and Technology (AZimuth)*. North Holland, **1997**, 45–50.
23. Caldiño, U.; Lira, A.; Meza-Rocha, A. N.; Camarillo, I.; Lozada-Morales, R. *J. Lumin.* **2018**, *194*, 231–239. DOI: <http://dx.doi.org/10.1016/j.jlumin.2017.10.028>.
24. Bünzli, J. C. G. *Handb. Phys. Chem. Rare Earths*. **2016**, *50*, 141–176. DOI: <http://dx.doi.org/10.1016/bs.hpcr.2016.08.003>.
25. Yen, W.M.; Shionoya, S.; Yamamoto, H., in: *Phosphor Handbook*. CRC Press/Taylor and Francis, **2007**, 149–151.